EBioMedicine 44 (2019) 150–161

Contents lists available at ScienceDirect

EBioMedicine

journal homepage: www.ebiomedicine.com

EBioMedicine
Published by THE LANCET

FOX-A1 contributes to acquisition of chemoresistance in human lung adenocarcinoma *via* transactivation of SOX5

Dongqin Chen [a,b,c,1], Rui Wang [c,1], Chen Yu [a,1], Fei Cao [b], Xuefeng Zhang [d,e], Feng Yan [a], Longbang Chen [c], Hong Zhu [b,*], Zhengyuan Yu [b,*], Jifeng Feng [a,**]

[a] Department of Medical Oncology, Jiangsu Cancer Hospital&Jiangsu Institute of Cancer Research&The Affiliated Cancer Hospital of Nanjing Medical University, Nanjing, China
[b] Department of Medical Oncology, the First Affiliated Hospital of Soochow University, Suzhou, China
[c] Department of Medical Oncology, Nanjing General Hospital of Nanjing Military Command, School of Medicine, Nanjing University, Nanjing, China
[d] Wake Forest Institute for Regenerative Medicine, Wake Forest School of Medicine, Winston-Salem,USA
[e] Department of Urology, the First Affiliated Hospital of Soochow University, Suzhou, China

ARTICLE INFO

Article history:
Received 5 April 2019
Received in revised form 18 May 2019
Accepted 21 May 2019
Available online 27 May 2019

Keywords:
Lung adenocarcinoma
Chemoresistance
FOX-A1
SOX5

ABSTRACT

Background: Chemoresistance is a major obstacle for the effective treatment of lung adenocarcinoma (LAD). Forkhead box (FOX) proteins have been demonstrated to play critical roles in promoting epithelial-mesenchymal transition (EMT) and chemoresistance. However, whether FOX proteins contribute to the acquisition of EMT and chemoresistance in LAD remains largely unknown.

Methods: FOX-A1 expression was measured in LAD cells and tissues by qRT-PCR. The expression levels of EMT markers were detected by western blotting and immunofluorescence assay. The interaction between Sex determining region Y-box protein 5 (SOX5) and FOX-A1 was validated by chromatin immunoprecipitation sequence (ChIP-seq) and Chromatin immunoprecipitation (ChIP) assay. Kaplan-Meier analysis and multivariate Cox regression analysis were performed to analyze the significance of FOX-A1 and SOX5 expression in the prognosis of LAD patients.

Findings: FOX-A1 was upregulated in docetaxel-resistant LAD cells. High FOX-A1 expression was closely associated with a worse prognosis. Upregulation of FOX-A1 in LAD samples indicated short progression-free survival (PFS) and overall survival (OS). SOX5 is a new and direct target of FOX-A1 and was positively regulated by FOX-A1 in LAD cell lines. Knockdown of FOX-A1 or SOX5 reversed the chemoresistance of docetaxel-resistant LAD cells by suppressing cell proliferation, migration and EMT progress.

Interpretation: These data elucidated an original FOX-A1/SOX5 pathway that represents a promising therapeutic target for chemosensitizing LAD and provides predictive biomarkers for evaluating the efficacy of chemotherapies.

1. Introduction

Lung adenocarcinoma (LAD), representing one of the leading cause of cancer-related mortality, has become the main human malignant cancer and a predominant public health problem around the world [1–3]. Although alternative therapeutic methods for LAD patients have been expanded over the past decades, the 5-year survival rate of patients with LAD remains <20% [4]. Despite the great progress and a significant improvement have been made in new therapeutic strategies, chemotherapy is still the cornerstone for the treatment of advanced LAD patients [5–9]. Nevertheless, most LAD patients quickly undergo disease progression and eventually die of chemoresistance and metastasis. Thus, exploring the potential molecular mechanisms accounting for acquisition and maintenance of LAD chemoresistance has been an urgent need for the exploration of novel therapeutic targets for reversing chemoresistance to achieve a better prognosis for LAD patients.

Epithelial-mesenchymal transition (EMT), a developmental process that involves a loss of epithelial characteristics and acquisition of mesenchymal phenotypes, has recently been reported to play an essential

* Corresponding authors at: Department of Medical Oncology, Jiangsu Cancer Hospital & Jiangsu Institute of Cancer Research & The Affiliated Cancer Hospital of Nanjing Medical University, 42 Baiziting Road, Nanjing 210009, Jiangsu, China; Department of Medical Oncology, the First Affiliated Hospital of Soochow University, 899 Pinghai Road, Suzhou 215006, Jiangsu, China.
** Correspondence to: J. Feng, Department of Medical Oncology, Jiangsu Cancer Hospital&Jiangsu Institute of Cancer Research&The Affiliated Cancer Hospital of Nanjing Medical University, 42 Baiziting Road, Nanjing 210009, Jiangsu, China.
E-mail addresses: zhuhong_jasmine@suda.edu.cn (H. Zhu), strongeryy1985@163.com (Z. Yu), profjffeng@163.com (J. Feng).
[1] The authors contributed equally to this work.

https://doi.org/10.1016/j.ebiom.2019.05.046

Research in context

Evidence before this study

Chemoresistance is a major obstacle for the effective treatment of LAD. EMT has recently been reported to play an essential role in driving tumor progression and chemoresistance. FOX proteins have been demonstrated to promote EMT in tumor progression. However, whether FOX proteins contribute to the acquisition of EMT and chemoresistance in LAD remains largely unknown and necessitates further exploration.

Added value of this study

Exploring the potential molecular mechanisms accounting for acquisition and maintenance of LAD chemoresistance has been an urgent need for the exploration of novel therapeutic targets for reversing chemoresistance to achieve a better prognosis for LAD patients. These data contribute to reveal a promising therapeutic target for chemosensitizing LAD and provide predictive markers for evaluating the efficacy of chemotherapies.

Implications of all the available evidence

In this study, we present the first evidence that FOX-A1 plays pivotal roles in exacerbating the development of EMT, metastasis and chemoresistance of docetaxel-resistant LAD cells, and knockdown of FOX-A1 reverses EMT to MET, attenuates metastatic characteristics and reverses the chemoresistance of docetaxel-resistant LAD cells by silencing SOX5, which is identified as a new and direct target of FOX-A1. These data elucidate an original FOX-A1/SOX5 pathway that represents a promising therapeutic target for reversing EMT characteristics and chemoresistance of LAD, providing predictive markers for evaluating the efficacy of chemotherapies.

role in driving tumor progression, metastasis and chemoresistance [10–13]. Importantly, tumor cells with EMT phenotypes often exhibit enhanced motility, invasive abilities and chemoresistant characteristics, while the reversal of EMT to mesenchymal-epithelial transition (MET) can attenuate the metastatic and chemoresistant characteristics of tumor cells [12,14,15]. To further explore the mechanisms underlying acquired chemoresistance in LAD cells, the docetaxel-resistant SPC-A1 (SPC-A1/DTX) and H1299 (H1299/DTX) cell lines with acquired characteristics of EMT and enhanced capacities for invasion and migration, have previously been established *via* continuous exposure of the parental LAD cells (SPC-A1 and H1299) to docetaxel for >1 year until the cells acquired taxane (docetaxel and paclitaxel) resistance [16]. However, the potential mechanisms responsible for the acquisition of EMT characteristics and chemoresistance of docetaxel-resistant LAD cells have remained largely unclear and require further exploration.

Forkhead box (FOX) proteins make up a family of evolutionarily conserved DNA-binding proteins that regulate transcription and play pivotal roles in exacerbating the development and maintenance of EMT, tumor metastasis and chemoresistance [17]. FOXM1D promotes EMT and metastasis in colorectal cancer by inducing actin assembly and impairing E-cadherin expression [18]. Foxf2, which is elevated in mesenchymal-like metastatic lung cancer cells, induces EMT, invasion and metastasis of lung cancer cells by transcriptionally repressing E-cadherin and microRNA-200 [19]. Tyrosine kinase inhibitors activate the AKT/FOXM1/STMN1 pathway, promoting the acquisition of EMT characteristics and multidrug resistance in non-small cell lung cancer cells [20]. FOXM1 inhibition reverses the chemoresistance of paclitaxel-resistant nasopharyngeal carcinoma cells that have acquired EMT and multidrug-resistance phenotypes by blocking drug efflux and increasing the intracellular concentrations of paclitaxel [21]. Collectively, the pivotal roles of EMT in the induction of metastasis and chemoresistance in these solid tumors suggest that Fox proteins might be responsible for the acquisition of metastatic characteristics and chemoresistance in LAD.

Here, we present the first evidence that FOX-A1 plays pivotal roles in exacerbating the development of EMT, metastasis and chemoresistance of docetaxel-resistant LAD cells, and knockdown of FOX-A1 reverses EMT to MET, attenuates metastatic characteristics and reverses the chemoresistance of docetaxel-resistant LAD cells by silencing Sex determining region Y-box protein 5 (SOX5), which is identified as a new and direct target of FOX-A1. These data elucidate an original FOX-A1/SOX5 pathway that represents a promising therapeutic target for reversing EMT characteristics and chemoresistance of LAD, thus providing predictive markers for evaluating the efficacy of chemotherapies.

2. Materials and method

2.1. Ethics approval

This study was approved by the Review Board of Hospital Ethics Committee of Nanjing General Hospital of Nanjing Military Command (No. 2012-2-12-015, No. 2012-2-13-022, Nanjing General Hospital of Nanjing Military Command, Nanjing University, China) and conducted in accordance with the Declaration of Helsinki, and written informed consent was obtained from all patients before specimen collection.

2.2. Cell lines, mice and chemical reagents

Human bronchial epithelioid cell (HBE) and LAD cells (SPC-A1, H1299, A549, H1650, Calu, H1975, H3122, H157, HCC827 and CAL-12 T) were obtained from Shanghai Institute of Cell Biology (Shanghai, China). Docetaxel-resistant SPC-A1 (SPC-A1/DTX) and H1299 (H1299/DTX) cells were previously established *via* continuous exposure of the parental LAD cells (SPC-A1 and H1299) to docetaxel for >1 year until the cells acquired taxane (docetaxel and paclitaxel) resistance [16]. Then, the docetaxel-resistant cells were preserved in 50.0 μg/L docetaxel.

The 4–6-week-old BALB/c athymic nude mice (76, male, 18-20 g, specific pathogen-free, SPF) were provided by the Department of Comparative Medicine of Nanjing Jinling Hospital (Nanjing University, China) and maintained in laminar flow cabinets under SPF conditions. Mouse experiments were conducted in accordance with the approval of the Institutional Committee for Animal Research of Nanjing Jinling Hospital (Nanjing University, China). The 4–6-week-old BALB/c athymic nude mice were housed in SPF facility. Environmental conditions were a temperature of 26-28 °C, humidity of 40%–60%, and a 10:14 light:dark cycle with lights on at 08:00 and off at 18:00. The mice were housed in 97cm^2 cages (Plastic cages with sealed air filter) placed in laminar flow cabinets and fed *ad libitum* mice maintenance food and water. The bedding material was grinded corn stalks. The cages were cleaned once a week. All materials (feed, water and other materials) that come into contact with mice was sterilized. Mice were sacrificed using carbon dioxide euthanasia. Docetaxel was purchased from Sigma Chemical Co. (St. Louis, MO, United States of America), prepared with dimethylsulfoxide and diluted in phosphate-buffered saline (PBS) to the required concentrations according to each experiment.

2.3. Patients

LAD tissues were obtained from patients with advanced LAD at the Department of Medical Oncology of Nanjing Jinling Hospital between

March 2005 and January 2008. A total of 52 patients met all the criteria as follows: diagnosed with primary LAD with one or more measurable lesions; clinical stage of IIIB-IV; first-line chemotherapies with docetaxel 75 mg/m^2 and cisplatin 100 mg/m^2 or carboplatin with an AUC of 6 mg/mLmin, administered every 3 weeks for amaximum of 5 cycles. Clinical stage was assessed in accordance with the American Joint Committee on Cancer. Tumor response was evaluated by computed tomography at every third cycle of chemotherapy in accordance with the Response Evaluation Criteria in Solid Tumorsas a complete response (CR), partial response (PR), stable disease (SD) or progressive disease (PD). CR and PR were regarded as "sensitive", while SD and PD were regarded as "insensitive". Tissue samples were snap-frozen and stored in liquid nitrogen until RNA extraction. The tissue acquisition was approved by the Hospital Ethics Committee of Nanjing Jinling Hospital (Nanjing University, China) and written informed consent was obtained from all patients.

2.4. In vitro chemosensitivity assay

The chemosensitivity assay was performed using the cell counting kit-8 (CCK-8) (Dojindo, Kumamoto, Japan) assay in accordance with the manufacturer's instructions. Briefly, 3000 LAD cells were plated in 96-well plates 24 h after transfection. Next, the cells were treated with different doses of docetaxel and cultured for 48 h. Then, CCK-8 solution was added and incubated at 37 °C for 4 h. The absorbance was detected at 450 nm with a microplate reader (Bio-Rad, USA).

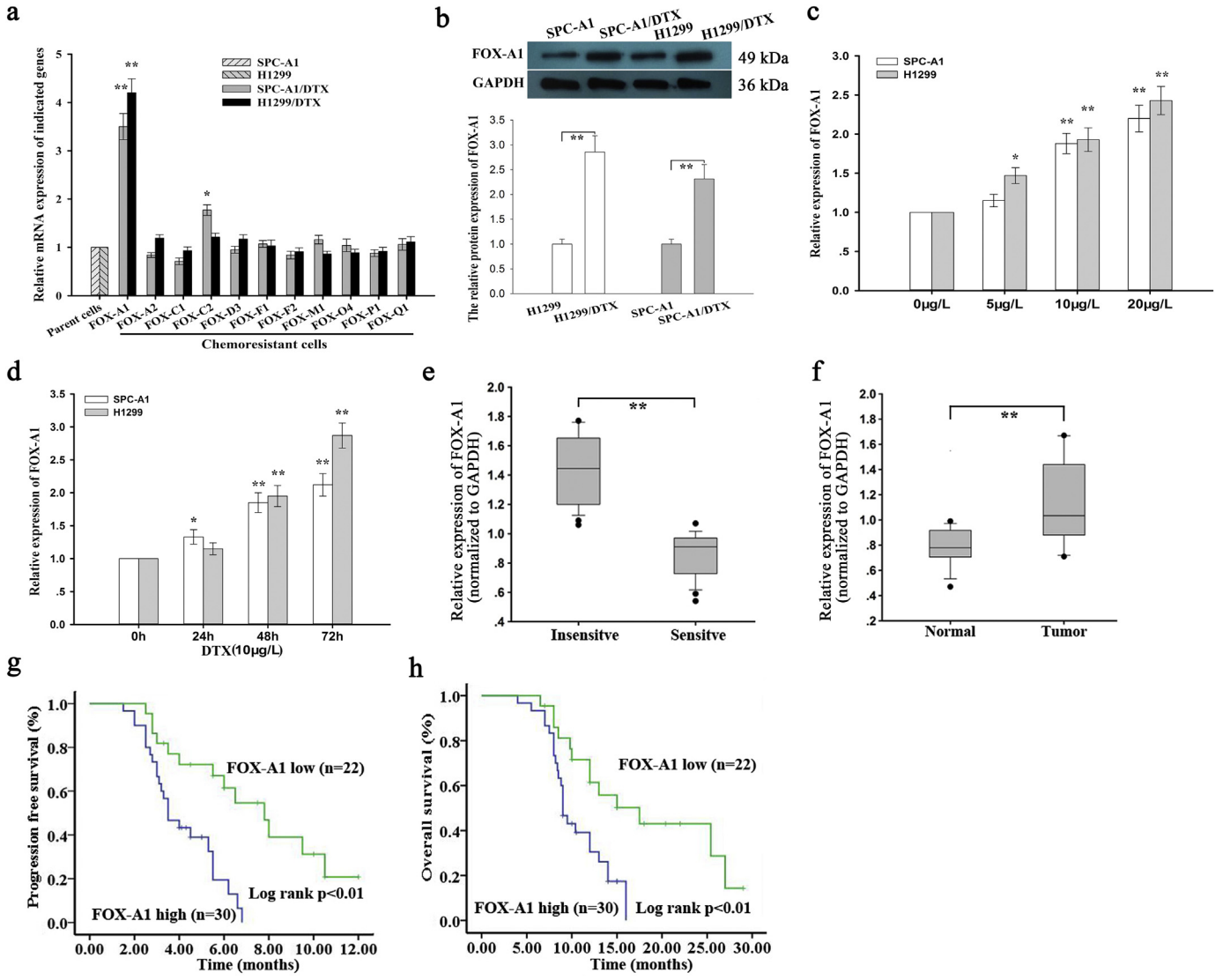

Fig. 1. FOX-A1 is upregulated in docetaxel-resistant LAD cells and insensitive LAD tissues and correlated with a poor prognosis of LAD patients. a, Relative expression of Forkhead box (Fox) genes in parental (SPC-A1 and H1299) and docetaxel-resistant LAD cells (SPC-A1/DTX and H1299/DTX) was determined by quantitative real-time PCR (qRT-PCR). GAPDH was used as an internal control. $^{**}P < 0.01$. Data are representative of at least three independent experiments (means±standard deviation). b, Western blotting was used to detect protein expression of FOX-A1 in parental and docetaxel-resistant LAD cells. GAPDH was used as an internal control. $^{**}P < 0.01$. Data are representative of at least three independent experiments (means± standard deviation). c, FOX-A1 gene expression was determined by qRT-PCR in parental LAD cells treated with different concentrations of DTX for 48 h. U6 was used as an internal control. $^{*}P < 0.05$, $^{**}P < 0.01$. Data are representative of at least three independent experiments (means±standard deviation). d, qRT-PCR detection of FOX-A1 gene expression in parental LAD cells treated with DTX at different time points. U6 was used as an internal control. $^{*}P < 0.05$, $^{**}P < 0.01$. Data are representative of at least three independent experiments (means±standard deviation). e, FOX-A1 expression detected by qRT-PCR in insensitive LAD tissues (CR + PR; n = 24) and sensitive LAD tissues (SD + PD; n = 28). GAPDH was used as an internal control. The cut-off value (0.959) of FOX-A1 mRNA expression in tumor tissues was determined by a receiver operating characteristic (ROC) curve.$^{**}P < 0.01$. f, FOX-A1 expression levels in normal lung tissues (n = 18) and LAD tissues (n = 52). FOX-A1 expression was detected by qRT-PCR. GAPDH was used as an internal control. $^{**}P < 0.01$. g, Kaplan-Meier analysis of the correlation between FOX-A1 expression and progression-free survival (PFS) of LAD patients. $^{**}P < 0.01$. h, Kaplan-Meier analysis of the association between FOX-A1 expression and overall survival (OS) of LAD patients.$^{**}P < 0.01$.

2.5. RNA extraction, quantitative real-time reverse-transcription polymerase chain reaction (qRT-PCR), western blotting, immunofluorescence assay, colony formation assay, flow cytometric analysis and dual luciferase reporter assay

RNA extraction, qRT-PCR, western blotting, immunofluorescence, colony formation, *in vitro* transwell, flow cytometric and dual luciferase reporter assays were performed as previously described in our work [16,22]. The primer pairs for the FOX genes and SOX5 are presented in Supplementary Table 1. Primary antibodies against cleaved caspase-3 (1:1000, rabbit IgG), caspase-3 (1:1000, rabbit IgG), β-actin (1:1000, rabbit IgG), GAPDH (1:1000, rabbit IgG), FOX-A1 (1:1000, rabbit IgG), E-cadherin (1:1000, rabbit IgG), N-cadherin (1:1000, rabbit IgG) and Vimentin (1:1000, rabbit IgG) were purchased from Cell Signaling Technologies of USA. Primary antibodies against SOX5 (1:1000, rabbit IgG) was purchased from Millipore of Hong Kong.

2.6. Construction of plasmids and cell transfection

The primer pairs used for the sh-control, sh-FOX-A1#1, sh-FOX-A1#2, sh-FOX-A1#3, sh-SOX5#1, sh-SOX5#2, sh-SOX5#3, pcDNA-FOX-A1 and pcDNA-SOX5 are presented in Supplementary Table 2. The human SOX5 promoter construct (−1990/0 SOX5) was generated from genomic DNA according to the sequence (−1990/0) of the 5′-flanking region of the human SOX5 gene. Then, the region was amplified by PCR and cloned into the pGL3-basic vector (Promega, San Luis, CA, USA) at *Kpn*I and *Hind*III sites. The 5′-flanking deletion promoter constructs (−1849/0 SOX5, −1592/0 SOX5, −1520/0 SOX5, −1490/0 SOX5, −470/0 SOX5) were generated with the −1990/0 SOX5 construct as a template and similarly cloned. Mutation of FOX-A1 binding site-mutant constructs was generated using a QuikChange XL site-directed mutagenesis kit from Stratagene (La Jolla, CA, USA). All primer sequences are presented in Supplementary Table 3. All vectors were confirmed by DNA sequencing. Cells were transfected with Turbofect Transfection Reagent (Thermo Scientific, USA) according to the manufacturer's instructions.

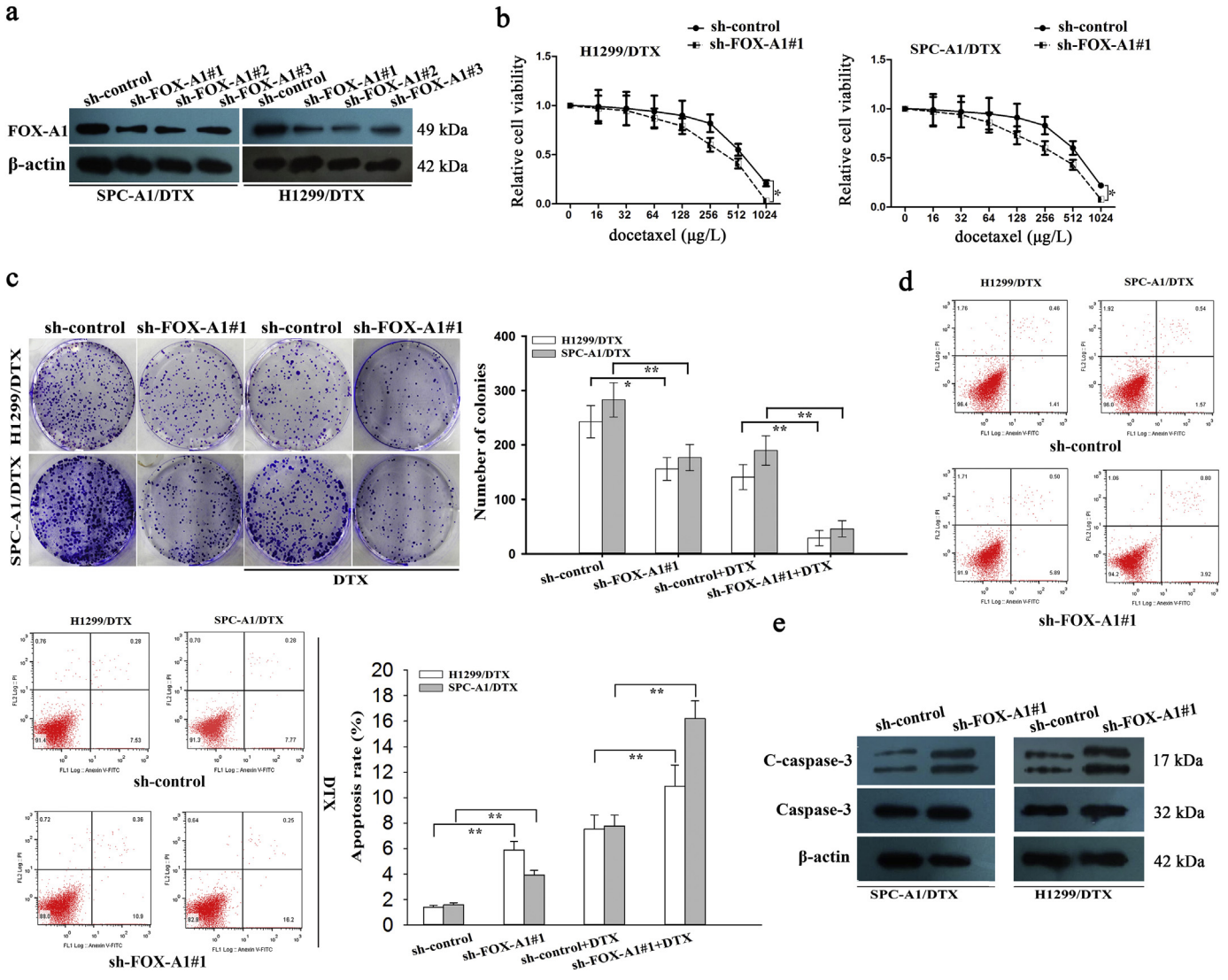

Fig. 2. FOX-A1 contributes to docetaxel resistance of LAD cells *in vitro*. a, Western blotting detection of FOX-A1 in docetaxel-resistant LAD cells transfected with sh-FOX-A1#1, sh-FOX-A1#2, sh-FOX-A1#3 or control. β-actin was used as a control. b, A CCK-8 assay was conducted to detect the IC_{50} values of DTX in sh-control (or sh-FOX-A1#1)-transfected docetaxel-resistant LAD cells. $^{*}P < 0.05$. c, A colony formation assay was performed to detect the proliferation ability of sh-control (or sh-FOX-A1#1)-transfected docetaxel-resistant LAD cells treated without (or with) DTX (50 μg/L). $^{*}P < 0.05$, $^{**}P < 0.01$. d, Flow cytometric analysis of the early apoptosis rate of sh-control (or sh-FOX-A1#1)-transfected docetaxel-resistant LAD cells treated without (or with) DTX (50 μg/L). $^{**}P < 0.01$. e, Western blotting was used to detect cleaved caspase-3 (C-caspase-3) and caspase-3 in sh-control (or sh-FOX-A1#1)-transfected docetaxel-resistant LAD cells. β-actin was used as an internal control. Data represent the average of three independent experiments (means±standard deviation).

2.7. Xenograft transplantation

The mice were randomly allocated to four groups (sh-control/sh-FOX-A1#1 or sh-control/sh-SOX5#3) with random number table. The experimenters were blinded to the docetaxel treatment and tumor volume measurement. Approximately 2×10^6 SPC-A1/DTX cells stably transfected with sh-control, sh-FOX-A1#1 or sh-SOX5#3 vector were suspended in 100 μL of phosphate-buffered saline and injected into the flanks of nude mice (n = 19, The 4–6-week-old BALB/c athymic nude mice were randomly allocated to sh-control, sh-FOX-A1#1 or sh-SOX5#3). Tumor volume was determined using the eq. $V = a \times b^2 \times 0.5$ (mm^3, a = largest diameter, b = perpendicular diameter). Once the tumor volume reached approximately 50 mm^3, 1.0 mg/kg docetaxel (1.0 mg/kg, one dose every other day, three doses in total) was administered by intraperitoneal injection [22]. 36 mice were sacrificed for subsequent studies on day 30, while the other 40 mice were maintained for further OS studies. Ki67, proliferating cell nuclear antigen (PCNA) staining and TUNEL staining were performed according to the manufacturer's instructions. Spots were examined independently by two observers blinded to treatment group. Proliferative activity was assessed by the percentage of positive tumor cells. For the OS studies, Cumulative survival probability curves were plotted with a Kaplan-Meier method and compared using a log-rank test. Mice were monitored twice daily for health status and there were no adverse events observed.

2.8. ChIP and ChIP-seq assay

The ChIP assay was performed using Immunoprecipitation Assay Kits (Millipore, USA) as described previously in our work [22]. The antibody against FOX-A1 (1:50, rabbit IgG) was purchased from Cell Signaling Technologies of USA. Eluted DNA fragments were analyzed by qRT-PCR. The primers used in the ChIP assay are provided in Supplementary Table 4. DNA libraries for Illumina cluster generation were performed as previously described [23,24]. Eluted DNA fragments were subjected to sequencing with Illumina HiSeq 2000 according to the

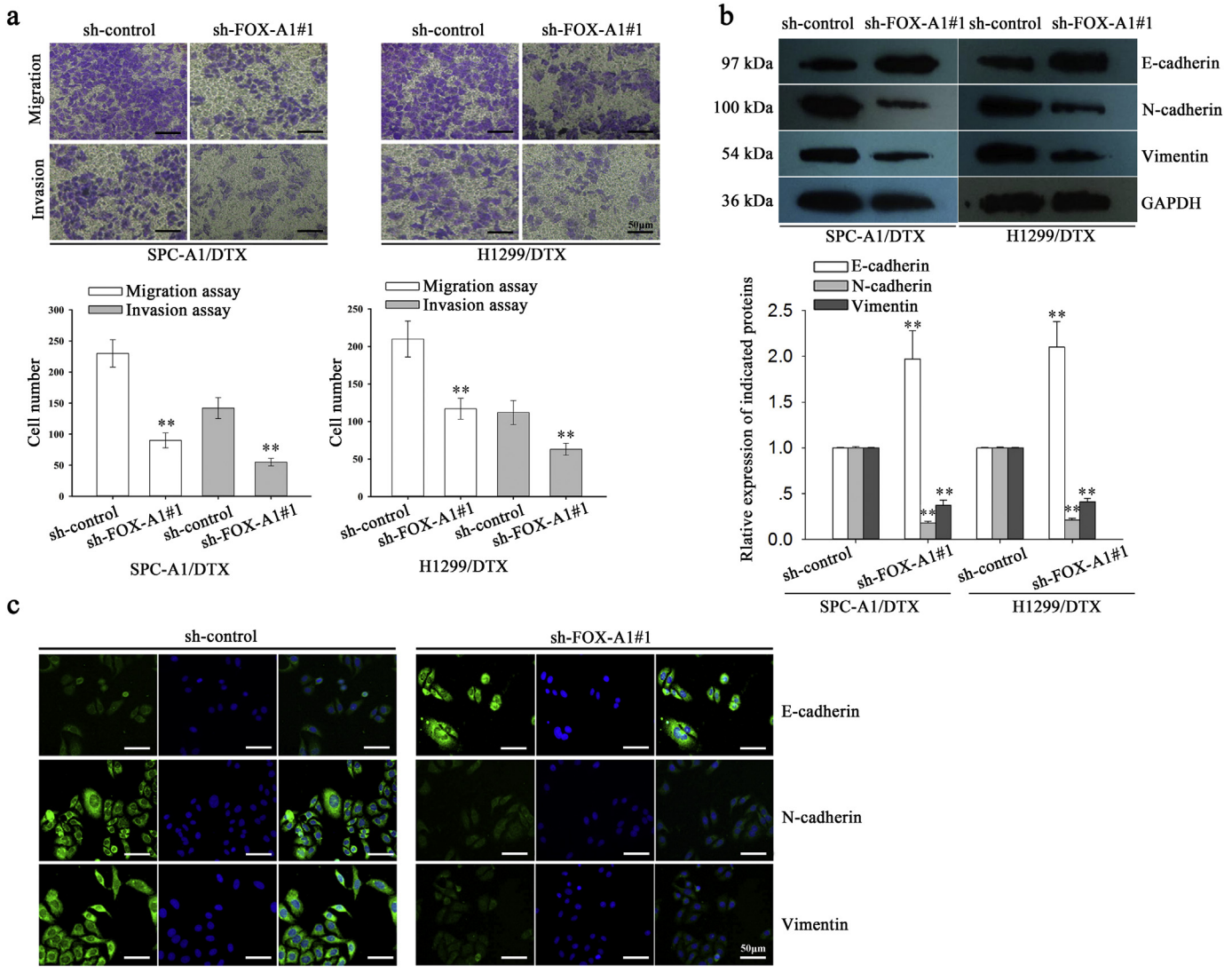

Fig. 3. FOX-A1 promotes migration, invasion and EMT of docetaxel-resistant LAD cells. a, A transwell assay was conducted to detect the migration and invasion of docetaxel-resistant LAD cells treated with sh-control or sh-FOX-A1#1 vectors. Migrated and invaded cells were calculated in five random fields of view at 100× magnification. A histogram displays the average number of migrated and invaded cells per field of view. Scar bar: 50 μm. $^{**}P < 0.01$. Data are presented as means±standard deviation. b, Western blotting was performed to detect the protein expression of an epithelial marker (E-cadherin) and mesenchymal markers (N-cadherin and Vimentin) in docetaxel-resistant LAD cells treated with sh-control or sh-FOX-A1#1 vectors. GAPDH was used as an internal control. $^{**}P < 0.01$. Data are presented as means±standard deviation. c, Immunofluorescence staining was used to detect the expression of an epithelial marker (E-cadherin) and mesenchymal markers (N-cadherin and Vimentin) in docetaxel-resistant LAD cells (SPC-A1/DTX) treated with sh-control or sh-FOX-A1#1 vectors. Scar bar: 50 μm.

manufacturer's protocol. ChIP-Seq analysis was performed as previously described with modifications [25,26].

2.9. Statistical analysis

SPSS software (version 17.0, SPSS Inc., Chicago, IL, USA) was utilized for statistical analysis. The data are presented as the means±standard deviation of at least three independent experiments. One-way ANOVA was performed to analyze multiple group comparisons of quantitative data, and the Student's *t*-test was performed to analyze two-group comparisons of quantitative data. The Chi-square test was used for categorical data. Cumulative survival probability curves were plotted with a Kaplan-Meier method and compared using a log-rank test. A Cox proportional hazards regression model was used to determine prognostic factors of PFS and OS. Correlations were confirmed by linear regression analysis. $^{*/\#}P < .05$ was considered statistically significant.

3. Results

3.1. FOX-A1 is upregulated in docetaxel-resistant LAD cells and insensitive LAD tissues and correlated with a poor prognosis of LAD patients

Recent studies have demonstrated that acquired chemoresistance often results in failure of therapies, tumor metastasis and relapse. To explore the underlying mechanisms of acquired docetaxel resistance in LAD cells, we have previously established docetaxel-resistant SPC-A1 (SPC-A1/DTX) and H1299 (H1299/DTX) cell lines *via* continuous exposure of the parental LAD cells (SPC-A1 and H1299) to docetaxel for more than one year until the cells had acquired taxane resistance [16]. Previously, we have confirmed that the docetaxel-resistant LAD cells acquired EMT phenotypes and showed increased invasion and migration capacities [16]. However, the potential mechanisms associated with the docetaxel-resistance of LAD cells remain largely unknown

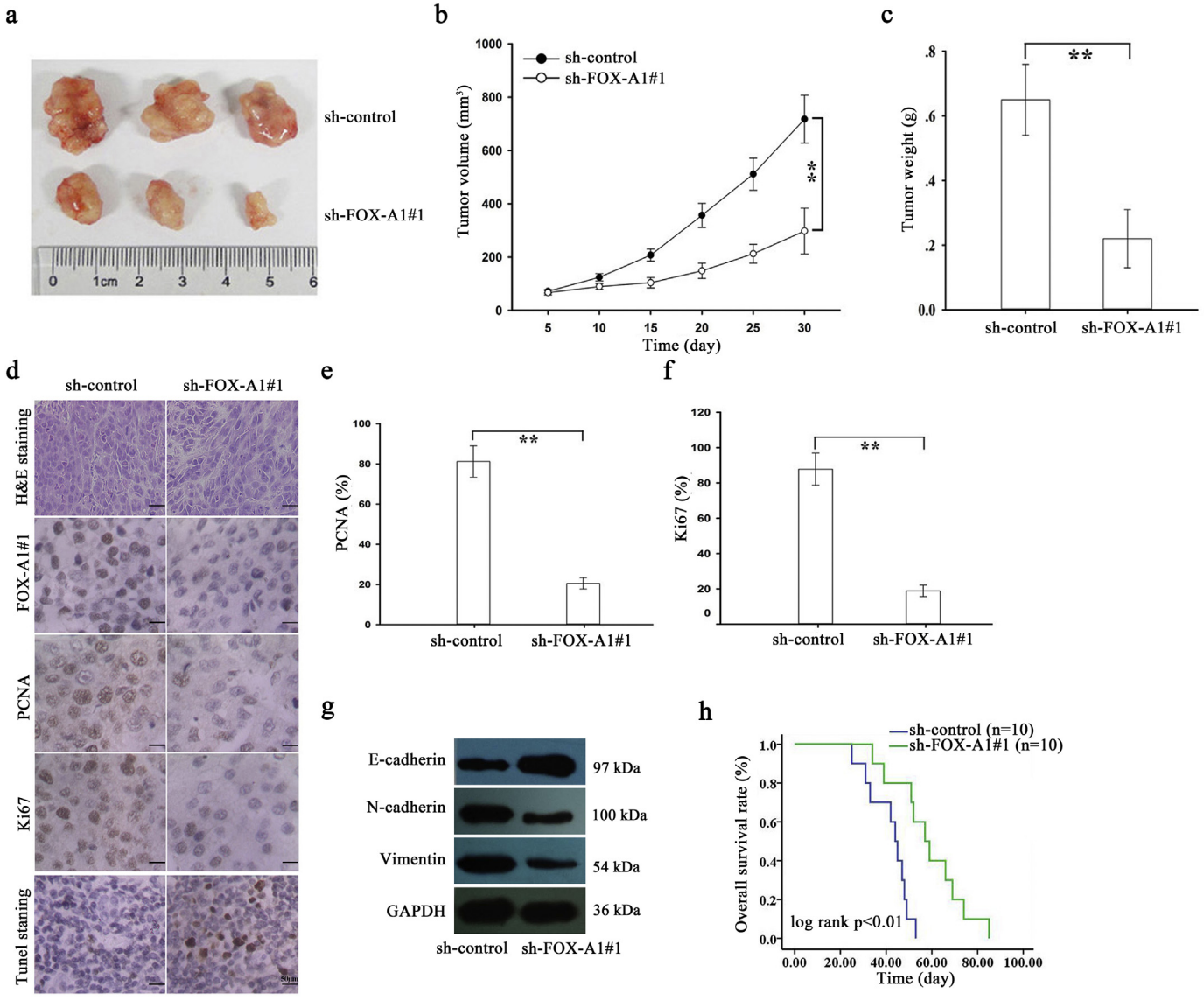

Fig. 4. Suppression of FOX-A1 enhances the *in vivo* chemosensitivity of docetaxel-resistant LAD cells to DTX. a, Tumor growth was assessed by the tumor volume in nude mice that were subcutaneously transplanted with sh-control (or sh-FOX-A1#1)-transfected SPC-A1/DTX cells combined with DTX treatment. The data are displayed as means±standard deviation. Representative photographs of tumors are provided at 30 days after inoculation. b-c, Tumor volume and weight of xenograft tumors at the end of the treatment period. $^{**}P < 0.01$. d, H&E staining, immunohistochemical staining of FOX-A1, proliferating cell nuclear antigen (PCNA) and Ki67 staining and TUNEL staining were performed using tumors collected at 30 days after inoculation. Scar bar: 50 μm. e-f, The positive rate of PCNA and Ki67 expression in tumors developed from sh-control (or sh-FOX-A1#1)-transfected SPC-A1/DTX cells combined with DTX treatment. $^{**}P < 0.01$. g, The level of E-cadherin, N-cadherin and Vimentin in sh-FOX-A1#1 group and sh-control group. h, Kaplan-Meier analysis of the OS of nude mice that were subcutaneously transplanted with sh-control (or sh-FOX-A1#1)-transfected SPC-A1/DTX cells combined with DTX treatment.$^{**}P < 0.01$. Data are presented as means± standard deviation.

and necessitate further exploration. FOX proteins, making up a family of evolutionarily conserved transcriptional regulators, play important roles in various biological processes, including EMT, tumor invasion and metastasis and chemoresistance.

First, qRT-PCR was performed to measure mRNA expression of Fox genes in parental and docetaxel-resistant LAD cells. As shown in Fig. 1a, FOX-A1 was significantly upregulated in both docetaxel-resistant LAD cells compared with the parental LAD cells. Similarly, the protein level of FOX-A1 was also higher in docetaxel-resistant LAD cells compared with the parental LAD cells (Fig. 1b). Interestingly, FOX-A1 was upregulated in the parental LAD cells induced by docetaxel in a dose- and time-dependent manner (Fig. 1c–d). Additionally, cell lines used in this study are resistant to multidrug. As presented in Supplementary Fig. 7a, knockdown of FOX-A1 also reduced the resistance of SPC-A1/DTX and H1299/DTX cell lines to cisplatin (CDDP) and paclitaxel (PTX). Similarly, we also examined the expression level of FOX-A1 in cells treated with CDDP or PTX in a dose- or time-dependent manner. It was found that FOX-A1 expression was gradually increased in cells treated CDDP or PTX in a dose- or time-dependent manner (Supplementary Fig. 8a-b). Furthermore, 52 LAD tissues obtained from patients who had received docetaxel-based chemotherapies were divided into insensitive LAD tissue (complete or partial response, CR + PR; n = 24) and sensitive LAD tissue (stable or progressive disease, SD + PD; n = 28) groups. qRT-PCR was performed to detect FOX-A1 expression in the two groups and revealed that FOX-A1 was significantly upregulated in insensitive LAD tissues compared with sensitive LAD tissues (Fig. 1e and Supplementary Fig. 6a). Furthermore, relative higher expression level of FOX-A1 was examined in tumor tissues compared with normal lung tissues (Fig. 1f and Supplementary Fig. 6b). Next, a receiver operating characteristic (ROC) curve analysis was performed to determine the optimal cut-off values for the expression level of FOX-A1, which was 0.959 in LAD tissues. Interestingly, high FOX-A1

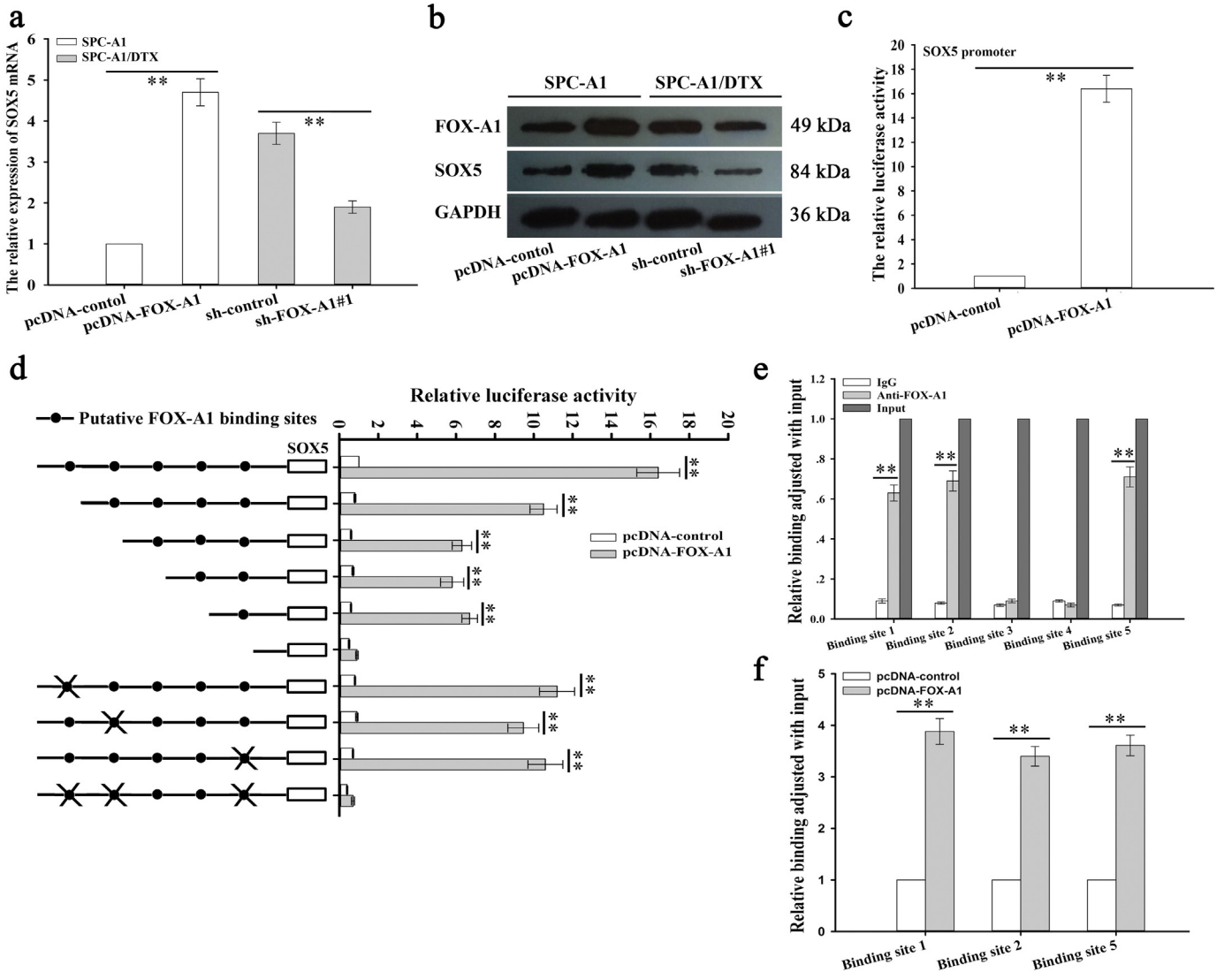

Fig. 5. SOX5 is identified as a direct target of FOX-A1. a-b, FOX-A1 upregulated SOX5 expression. SPC-A1 and SPC-A1/DTX cells were infected with pcDNA-FOX-A1 (or pcDNA-control) or sh-FOX-A1#1 (or sh-control), and the mRNA and protein expression of SOX5 were measured by qRT-PCR and western blotting. GAPDH was used as an internal control. $^{**}P < 0.01$. c, FOX-A1 transactivated SOX5 promoter activity. A SOX5 promoter luciferase construct, (−1990/0)SOX5, was cotransfected with pcDNA-FOX-A1 (or pcDNA-control), and the promoter activity was measured using a luciferase reporter assay. $^{**}P < 0.01$. d, Three FOX-A1 binding sites were identified in the SOX5 promoter. Serially truncated and site-mutated regions of the SOX5 promoter were constructed (left) and cloned into a pGL3-basic vector. These luciferase reporter vectors were then transfected into SPC-A1/DTX cells co-transfected with Renilla luciferase and pcDNA-FOX-A1 (or pcDNA-control) vectors. Then, the relative luciferase activity was detected using a dual-luciferase reporter assay (right). $^{**}P < 0.01$. e, FOX-A1 bound to the SOX5 promoter *in vivo*. Chromatin immunoprecipitation (ChIP) assays were performed using SPC-A1/DTX cells with antibodies directly against FOX-A1 or IgG control. qRT-PCR was performed to analyze the immunoprecipitated DNA with primers for amplifying the sequences containing the putative FOX-A1-binding sites. $^{**}P < 0.01$. f, FOX-A1 increased FOX-A1 binding to the SOX5 promoter *in vivo*. ChIP assays were performed with antibodies directed against FOX-A1 in pcDNA-FOX-A1 (or pcDNA-control)-transfected SPC-A1/DTX cells. Immunoprecipitated DNA was detected using qRT-PCR with primers for amplifying the sequences containing the putative FOX-A1-binding sites. $^{**}P < 0.01$. Data are presented as means±standard deviation.

expression was closely associated with advanced clinical stage, worse tumor response, and poor tumor differentiation and prognosis (Supplementary Table 5). Kaplan-Meier analysis indicated that high FOX-A1 expression was associated with a shorter PFS and OS (Fig. 1g-h). Finally, high FOX-A1 expression was identified as an independent prognostic factor for poor PFS and OS in LAD patients by univariate and multivariate Cox regression analysis (Supplementary Table 6-7). Moreover, the expression of FOX-A1 was detected in all ten NSCLC cell lines and human normal bronchial epithelioid cell line. It was found that FOX-A1 was expressed at high level at ten NSCLC cell lines (Supplementary Fig. 7b). Then, we tested the effect of FOX-A1 to the docetaxel-resistance of other eight NSCLC cell lines. Interestingly, overexpression of FOX-A1 enhanced the half maximal inhibitory concentration (IC_{50}) value of all other eight NSCLC cell lines (Supplementary Fig. 7c).

3.2. FOX-A1 promotes chemoresistance, migration, invasion and EMT of docetaxel-resistant LAD cells

To further investigate the functional role of FOX-A1 in regulating the chemoresistance of docetaxel-resistant LAD cells, shRNA(sh)-FOX-A1#1, sh-FOX-A1#2, sh-FOX-A1#3 or sh-control vector was transfected into docetaxel-resistant LAD cells. The sh-FOX-A1#1 vector exhibited the highest interference efficiency (Fig. 2a). Considering the low expression level of FOX-A1 in parental LAD cells, we overexpressed it by transfecting with pcDNA-FOX-A1 or empty vector (NC) (Supplementary Fig. 4a). The IC_{50} values for docetaxel in sh-FOX-A1#1 (or sh-control)-transfected docetaxel-resistant LAD cells (SPC-A1/DTX and H1299/DTX) were then detected using a CCK-8 assay. The IC_{50} values of docetaxel in sh-FOX-A1#1-transfected SPC-A1/DTX and H1299/DTX cells (310.2 ± 31.3 μg/L and 391.5 ± 35.8 μg/L) were significantly lower than those in sh-control-transfected SPC-A1/DTX and H1299/DTX cells (590.2 ± 58.4 μg/L and 642.4 ± 66.3 μg/L) (Fig. 2b). The IC_{50} value of parental cells transfected with FOX-A1 expression vector was significantly higher than those transfected with empty vector (Supplementary Fig. 4b). Next, downregulation of FOX-A1 significantly suppressed the colony formation capacity of SPC-A1/DTX and H1299/ DTX cells *in vitro* (Fig. 2c). Then, a flow cytometric analysis was used to detect early apoptosis and indicated that inhibition of FOX-A1 increased early apoptosis in sh-FOX-A1#1-transfected SPC-A1/DTX and H1299/DTX cells compared with sh-control-transfected SPC-A1/DTX and H1299/DTX cells (Fig. 2d). Moreover, western blotting to detect cleaved-caspase-3 indicated that the cleaved-caspase-3 protein level

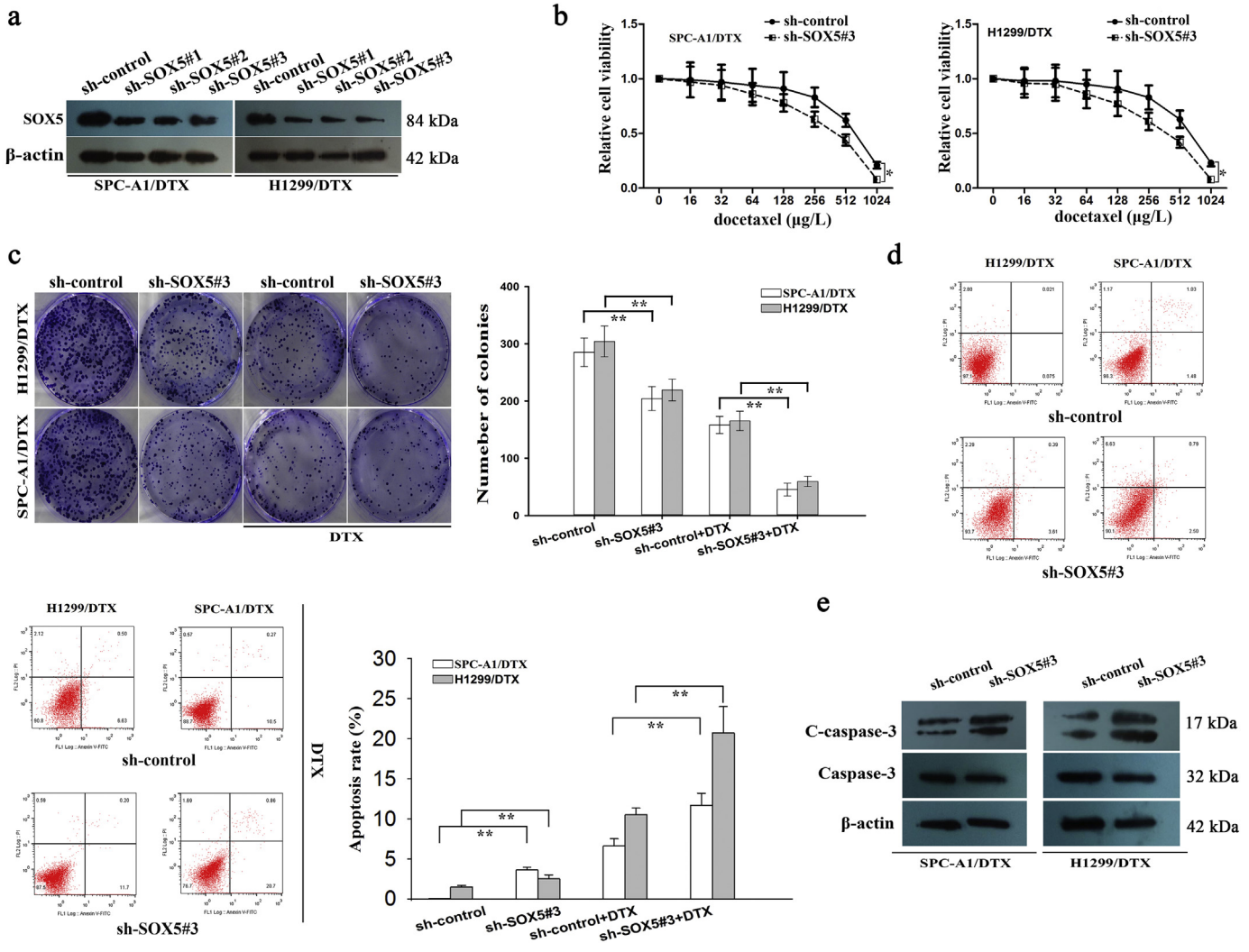

Fig. 6. SOX5 is responsible for docetaxel resistance of LAD cells *in vitro*. a, Western blotting detection of SOX5 in docetaxel-resistant LAD cells transfected with sh-SOX5#1, sh-SOX5#2, sh-SOX5#3 or control. β-actin was used as an internal control. b, A CCK-8 assay was performed to detect the IC_{50} values of DTX in sh-control (or sh-SOX5#3)-transfected docetaxel-resistant LAD cells. $^{*}P < 0.05$. c, A colony formation assay was conducted to detect the proliferation ability of sh-control (or sh-SOX5#3)-transfected docetaxel-resistant LAD cells treated without (or with) DTX (50 μg/L). $^{**}P < 0.01$. d, Flow cytometric analysis of the early apoptosis rate of sh-control (or sh-SOX5#3)-transfected docetaxel-resistant LAD cells treated without (or with) DTX (50 μg/L). $^{**}P < 0.01$. e, Western blotting was used to detect cleaved caspase-3 (C-caspase-3) and caspase-3 in sh-control (or sh-SOX5#3)-transfected docetaxel-resistant LAD cells. β-actin was used as an internal control. Data represent the average of three independent experiments (means±standard deviation).

was significantly upregulated in sh-FOX-A1#1-transfected SPC-A1/DTX and H1299/DTX cells in comparison to the control group (Fig. 2e). Additionally, overexpression of FOX-A1 promoted the colony formation ability and suppressed apoptosis in parental LAD cells (Supplementary Fig. 4c–d).

EMT plays important roles in the promotion of chemoresistance, migration and invasion of docetaxel-resistant LAD cells. As shown in Fig. 3a, the transwell assay and Matrigel transwell assay indicated that suppression of FOX-A1 could significantly inhibit the migration and invasion of SPC-A1/DTX and H1299/DTX cells. A typical characteristic of EMT is increased expression of mesenchymal markers such as N-cadherin and Vimentin and decreased expression of epithelial markers such as E-cadherin. Next, western blotting was performed to evaluate the expression of epithelial and mesenchymal molecular markers and indicated that expression of an epithelial protein marker (E-cadherin) was dramatically increased in sh-FOX-A1#1-transfected SPC-A1/DTX and H1299/DTX cells compared with the control group (Fig. 3b). Conversely, the mesenchymal markers (N-cadherin and Vimentin) were significantly reduced in sh-FOX-A1#1-transfected SPC-A1/DTX and H1299/DTX cells compared with the control group. Furthermore, an immunofluorescence assay was conducted to detect the expression of epithelial and mesenchymal molecular markers. The expression of E-cadherin was significantly increased while the expression of N-cadherin and Vimentin was dramatically decreased in sh-FOX-A1#1-transfected SPC-A1/DTX cells compared with the control group (Fig. 3c). These data indicated that inhibition of FOX-A1 reversed EMT to MET in docetaxel-resistant LAD cells. Therefore, we confirmed the oncogenic role of FOX-A1 in LAD progression and the effects on the chemoresistance of docetaxel-resistant LAD cells.

Next, *in vivo* experiments were further conducted to determine the role of FOX-A1 in the chemoresistance of docetaxel-resistant LAD cells to docetaxel. First, approximately 2×10^6 SPC-A1/DTX cells that were stably transfected with sh-control or sh-FOX-A1#1 vector were subcutaneously transplanted into nude mice. Once the tumor size had reached approximately 50 mm^3, docetaxel (1.0 mg/kg, one dose every other day, three doses in total) was administered, and the tumor volume was measured. Tumor volume in sh-control-transfected group was as follows: (day 5: 71.5 ± 6.6 mm^3, day 10: 124.1 ± 13.7 mm^3, day 15: 207.2 ± 22.6 mm^3, day 20: 356.5 ± 45.3 mm^3, day 25: 511.4 ± 60.4 mm^3, and day 30: 717.6 ± 89.5 mm^3, respectively) (Fig. 4b).

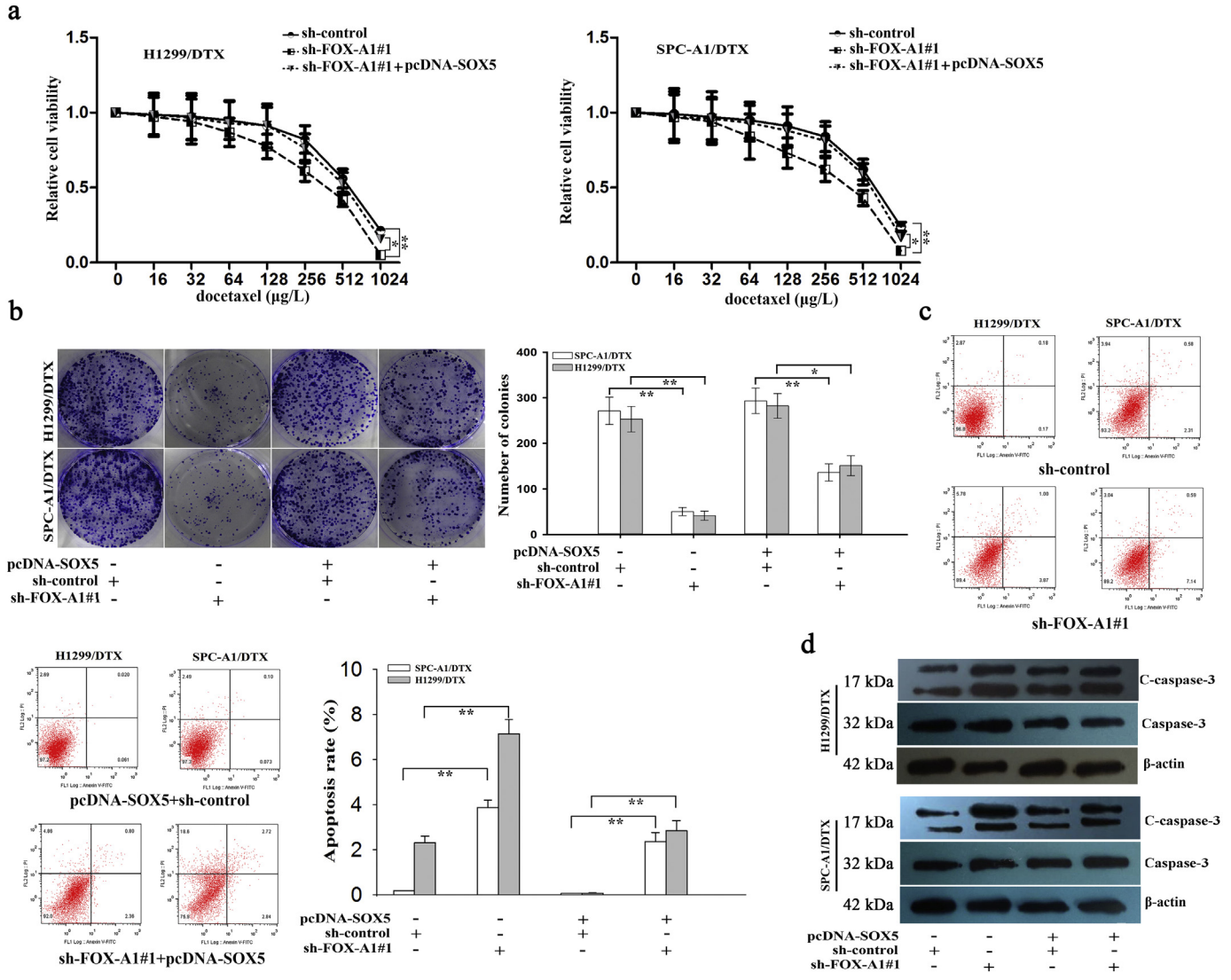

Fig. 7. FOX-A1 is involved in the docetaxel resistance of LAD cells partially in a SOX5-dependent manner. a, CCK-8 assay analysis of the IC_{50} values of DTX in sh-control (or sh-FOX-A1#1)-transfected docetaxel-resistant LAD cells co-transfected with pcDNA-SOX5. $^{*}P < 0.05$, $^{**}P < 0.01$. b, A colony formation assay was performed to detect the proliferation ability of sh-control (or sh-FOX-A1#1)-transfected docetaxel-resistant LAD cells co-transfected with pcDNA-SOX5. $^{*}P < 0.05$, $^{**}P < 0.01$. c, Flow cytometric analysis of the early apoptosis rate of sh-control (or sh-FOX-A1#1)-transfected docetaxel-resistant LAD cells co-transfected with pcDNA-SOX5. $^{*}P < 0.05$, $^{**}P < 0.01$. d, Western blotting was used to detect cleaved caspase-3 (C-caspase-3) and caspase-3 in sh-control (or sh-FOX-A1#1)-transfected docetaxel-resistant LAD cells co-transfected with pcDNA-SOX5. Data represent the average of three independent experiments (means±standard deviation).

Tumor volume in sh-FOX-A1#1-transfected group was as follows: (day 5: 66.4 ± 8.3 mm^3, day 10: 89.5 ± 10.1 mm^3, day 15: 103.7 ± 19.4 mm^3, day 20: 148.3 ± 28.9 mm^3, day 25: 212.4 ± 35.2 mm^3, and day 30: 297.5 ± 85.8 mm^3, respectively) (Fig. 4b). Tumor weight was 0.22 ± 0.09 g in sh-FOX-A1#1-transfected group. Tumor weight was 0.65 ± 0.11 g in sh-control-transfected group (Fig. 4c). The body weight of nude mice was measured and shown in Supplementary Fig. 7d. Next, immunohistochemical staining revealed that downregulation of FOX-A1 significantly decreased the positive rate of Ki67 and PCNA (Fig. 4d–f). The increased level of E-cadherin and decreased levels of N-cadherin and Vimentin were examined in sh-FOX-A1#1 group compared to the control group (Fig. 4g). TUNEL staining showed that apoptotic cells were increased in the sh-FOX-A1#1 group in comparison to the control group (Fig. 4d). Finally, Kaplan-Meier analysis of the OS data indicated that suppression of FOX-A1 was significantly associated with a longer OS in mice (Fig. 4h). Some proteins have been reported to be crucial regulators in the chemoresistance of human cancer cells. For example, ABCB1 (P-glycoprotein, MDR-1) has been verified to be an important DTX-resistant protein [27]. Here, we examined the protein level of ABCB1 in FOX-A1-overexpressed parental cell lines or FOX-A1-downregulated docetaxel-resistant cell lines. The protein level was not significantly changed (Supplementary Fig. 8c).

3.3. SOX5 is identified as a new and direct target of FOX-A1

ChIP sequencing data revealed that SOX5 might be a potential target of FOX-A1 (Supplementary Fig. 1a). The information of the 20 candidate genes is presented in Supplementary Table 8. Among which, SOX5 had highest peak score. According to the ChIP sequencing data, the GO enrichment analysis and KEGG pathway analysis were conducted (Supplementary Fig. 1b-c). To detect the potential role of SOX5 in the progression and chemoresiatance of LAD, we examined the expression of SOX5 in different LAD tissues. As shown in Supplementary Fig. 1d–e and Supplementary Fig. 6c–d, SOX5 was expressed higher in insensitive LAD tissues and tumor tissues. Kaplan-Meier survival curves indicated that high level of SOX5 was correlated with the low PFS and OS (Supplementary Fig. 1f–g). Finally, the positive expression association between SOX5 and FOX-A1 was analyzed in LAD tissues (Supplementary Fig. 1h). To further confirm the ChIP sequencing data, qRT-PCR and western blotting detection of mRNA and protein expression of SOX5 were performed in SPC-A1 or SPC-A1/DTX cells transfected with pcDNA-control (pcDNA-FOX-A1) or sh-control (sh-FOX-A1#1) and indicated that FOX-A1 could significantly upregulate SOX5 expression (Fig. 5a–b). Next, to further determine whether FOX-A1 could regulate SOX5 transcription, a SOX5 promoter luciferase construct, (−1990/0) SOX5, was cotransfected with pcDNA-FOX-A1 into SPC-A1/DTX cells. A luciferase reporter assay indicated that FOX-A1 could transactivate SOX5 promoter activity (Fig. 5c).

To further define the potential mechanisms by which FOX-A1 mediated SOX5 expression, the promoter region of the SOX5 gene was analyzed using open online databases (Consite and PROMO). Then, five putative complementary FOX-A1 binding sites were found and are depicted in the schematic of the human SOX5 promoter. Next, serially truncated and site-mutated regions of the SOX5 promoter were constructed and cloned into a pGL3-basic vector, and the luciferase reporter vectors were then co-transfected into SPC-A1/DTX cells with Renilla luciferase and pcDNA-control (or pcDNA-FOX-A1). A dual-luciferase reporter assay was then performed to measure the relative luciferase activity and demonstrated that the first, second and fifth FOX-A1 binding sites were responsible for transactivation of SOX5 by FOX-A1 (Fig. 5d). To further determine whether FOX-A1 interacted with the FOX-A1 binding sites *in vivo*, a ChIP assay was performed in SPC-A1/DTX cells using antibodies that directly targeted FOX-A1, and the results showed that FOX-A1 directly bound to the first, second and fifth FOX-A1 binding sites *in vivo* (Fig. 5e). Next, ChIP assay further demonstrated that the upregulation of FOX-A1 increased the binding of FOX-A1 to FOX-A1-binding sites within the SOX5 promoter (Fig. 5f). Collectively, SOX5 might be a new and direct target of FOX-A1.

3.4. Inhibition of SOX5 suppressed chemoresistance, migration, invasion and EMT of docetaxel-resistant LAD cells

The expression level of SOX5 was detected in parental LAD cells and docetaxel-resistant LAD cells. Consistent with FOX-A1, SOX5 was expressed higher in docetaxel-resistant LAD cells than that in parental cells (Supplementary Fig. 5a). To further understand the functional roles of SOX5, the vector containing sh-SOX5#1, sh-SOX5#2, sh-SOX5#3 or control was transfected into docetaxel-resistant LAD cells. The sh-SOX5#3 vector was confirmed to be the most efficient shRNA against SOX5 (Fig. 6a). Similarly, we overexpressed it in two parental cells by transfecting with pcDNA-SOX5 and empty vector (Supplementary Fig. 5b). Next, IC_{50} values of docetaxel detected using a CCK-8 assay

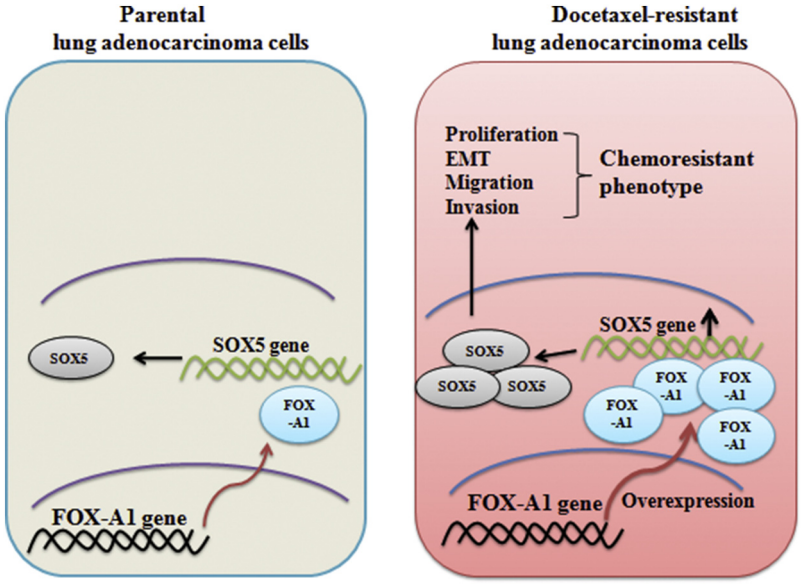

Fig. 8. Proposed model of the regulation of FOX-A1 by SOX5 between parental and docetaxel-resistant LAD cells. Compared with parental LAD cells, FOX-A1 was upregulated in docetaxel-resistant LAD cells, which resulted in the upregulation of its target gene SOX5 and subsequently contributed to cell proliferation, EMT, migration, invasion and chemoresistance.

in sh-SOX5#3-transfected SPC-A1/DTX and H1299/DTX cells (431.1 ± 47.3 μg/L and 415.7 ± 37.6 μg/L) were significantly lower than those in sh-control-transfected SPC-A1/DTX and H1299/DTX cells (615.4 ± 62.7 μg/L and 633.5 ± 57.6 μg/L) (Fig. 6b). The increased IC_{50} value was examined in parental cells transfected with pcDNA-SOX5 compared to cells transfected with empty vector (Supplementary Fig. 5c). Moreover, suppression of SOX5 significantly reduced the colony formation capacity of SPC-A1/DTX and H1299/DTX cells *in vitro* while promoted cell apoptosis (Fig. 6c–e). However, overexpression of SOX5 led to the opposite results in parental cells (Supplementary Fig. 5d–e).

Next, we focused on determining the effects of SOX5 on EMT, migration and invasion of docetaxel-resistant LAD cells. First, the transwell and Matrigel transwell assay indicated that suppression of SOX5 significantly inhibited the migration and invasion of SPC-A1/DTX and H1299/DTX cells (Supplementary Fig. 2a). Then, western blotting indicated that the expression of E-cadherin was significantly increased in sh-SOX5#3-transfected SPC-A1/DTX and H1299/DTX cells compared with the control group. Conversely, the expression levels of N-cadherin and Vimentin were significantly downregulated in sh-SOX5#3-transfected SPC-A1/DTX and H1299/DTX cells compared with the control group (Supplementary Fig. 2b). Next, the immunofluorescence assay indicated that E-cadherin was dramatically increased while N-cadherin and Vimentin were significantly decreased in sh-SOX5#3-transfected SPC-A1/DTX cells compared with the control group (Supplementary Fig. 2c). These data indicated the oncogenic role of SOX5 in the progression and chemoresistance of LAD *in vitro*.

For detection of the effect of SOX5 on the chemoresistance of docetaxel-resistant LAD cells to docetaxel *in vivo*, approximately 2×10^6 SPC-A1/DTX cells that were stably transfected with sh-control or sh-SOX5#3 vector were subcutaneously transplanted into nude mice. Once the tumor size had reached approximately 50 mm^3, docetaxel was administered, and the tumor volume was measured. As shown in Supplementary Fig. 3a–c, tumor volume in sh-control-transfected group was as follows: (day 5: 66.5 ± 7.1 mm^3, day 10: 115.4 ± 14.4 mm^3, day 15: 217.5 ± 20.4 mm^3, day 20: 351.3 ± 33.7 mm^3, day 25: 471.5 ± 45.5 mm^3, and day 30: 621.7 ± 65.8 mm^3, respectively). Tumor volume in sh-SOX5#3-transfected group was as follows: (day 5: 67.2 ± 6.4 mm^3, day 10: 82.5 ± 11.3 mm^3, day 15: 116.5 ± 12.6 mm^3, day 20: 147.8 ± 14.3 mm^3, day 25: 222.6 ± 21.3 mm^3, and day 30: 285.7 ± 32.5 mm^3, respectively). Tumor weight was 0.18 ± 0.06 g in sh-SOX5#3-transfected group. Tumor weight was 0.60 ± 0.09 g in sh-control-transfected group (Supplementary Fig. 3c). The body weight of nude mice in different groups was measured and illustrated in Supplementary Fig. 7d. Next, immunohistochemical staining revealed that inhibition of SOX5 significantly decreased the positive rate of Ki67 and PCNA (Supplementary Fig. 3d–f). TUNEL staining indicated that downregulation of SOX5 significantly increased the proportion of apoptotic cells (Supplementary Fig. 3d). Moreover, the increased level of E-cadherin and decreased levels of N-cadherin and Vimentin were examined in sh-SOX5#3 group (Supplementary Fig. 3g). Finally, Kaplan-Meier analysis revealed that low expression of SOX5 was significantly associated with a longer OS in mice (Supplementary Fig. 3h).

3.5. Upregulation of SOX5 partially abrogates the effects of knockdown of FOX-A1 on the enhanced chemosensitivity of docetaxel-resistant LAD cells

To further investigate the role of SOX5 in FOX-A1 signaling, rescue assays were carried out in two docetaxel-resistant LAD cells. Intriguingly, the IC_{50} values of DTX in sh-FOX-A1#1-transfected docetaxel-resistant LAD cells were partially abrogated by transfection with pcDNA/SOX5 (Fig. 7a). A colony formation assay revealed that the proliferation ability of the sh-FOX-A1#1-transfected docetaxel-resistant LAD cells was partially reversed by transfection with pcDNA/SOX5 (Fig. 7b). Additionally, early apoptosis and cleaved caspase-3 expression in sh-FOX-A1#1-transfected docetaxel-resistant LAD cells were partially abrogated by transfection with pcDNA/SOX5 (Fig. 7c–d). Previously, we have demonstrated that miR-451 regulated chemosensitivity of LAD cell lines. Here, we examined the potential regulatory relationship between miR-451 and FOX-A1/SOX5 axis. The results suggested that miR-451 and FOX-A1/SOX5 had no significant effect on each other (Supplementary Fig. 7e). Collectively, our research findings revealed that FOX-A1/SOX5 axis enhanced resistance of LAD cells to docetaxel (Fig. 8).

4. Discussion

Acquired chemoresistance often results in failure of therapies, tumor metastasis and relapse [28–30]. Chemoresistance of cancer cells is correlated with drug efflux and various molecular mechanisms. So far, the underlying mechanisms responsible for chemoresistance in LAD still remains largely unknown. EMT process plays a pivotal role in driving chemoresistance in many types of human tumors, which indicates that reversing EMT progress might result in a reversal of chemoresistant characteristics of LAD cells [31–33]. Previously, our research group has established docetaxel-resistant LAD cells that exhibited EMT-like characteristics and increased invasion phenotypes. In this study, we found that FOX-A1 was upregulated in docetaxel-resistant LAD cells. Prior studies have demonstrated that dysregulation of FOX-A1 plays crucial role in driving tumor progression [34]. Moreover, upregulation of FOX-A1 can promotes LAD metastasis by transcriptionally activating lysyl hydroxylase 2 [35]. FOX-A1 is overexpressed in several endocrine-resistant breast cancer cell lines and triggers endocrine resistance [36]. However, it is unclear whether FOX-A1 regulates docetaxel resistance of LAD cells. Through functional assays with drug treatment, we determined that FOX-A1 contributed to docetaxel resistance by promoting cell proliferation, migration and EMT progress.

Expression levels of FOX-A1 might be linked to the prognosis of patients in a context-dependent manner, depending on the tumor type-specific transcriptional program. In our present study, the expression of FOX-A1 was found to be higher in insensitive tissues and tumor tissues. Furthermore, high expression levels of FOX-A1 were significantly associated with a shorter PFS and OS. The correlation of FOX-A1 with clinical index of LAD patients was analyzed by Cox regression analysis. Thereby, FOX-A1 can be identified as an independent prognostic factor for LAD patients. FOX-A1 is a transcription factor that can induced the upregulation of genes [35]. To search for the downstream targets of FOX-A1 in LAD, ChIP-seq was conducted. After data analysis, we determined that SOX5 is a potential target of FOX-A1. Further mechanism investigation revealed that SOX5 was a direct transcriptional target of FOX-A1. Recently, SOX5 has been reported to play essential roles in stimulating the metastasis and progression of various tumors including breast cancer, prostate cancer, hepatocellular carcinoma and nasopharyngeal carcinoma [37,38]. SOX5 is known as an oncogene that can promote metastasis and EMT process in human prostate cancer [39,40]. Mechanistically, SOX5 activates Twist1 by binding to the Twist1 promoter, which results in the promotion of EMT of breast cancer cells [41]. However, little is known concerning whether SOX5 is involved in promoting EMT and chemoresistance of docetaxel-resistant LAD cells. In this study, we demonstrated that SOX5 is upregulated in docetaxel-resistant LAD cells. Knockdown of SOX5 reverses EMT to MET, attenuates metastatic characteristics and reverses the chemoresistance of docetaxel-resistant LAD cells. Similarly, the expression of SOX5 was higher in insensitive tissues and tumor tissues. Upregulation of SOX5 predicted poor prognosis in LAD patients. Interestingly, overexpression of SOX5 partially abrogates the effects of FOX-A1 knockdown on reversal of the chemoresistance of docetaxel-resistant LAD cells. Taken together, these data elucidate an original FOX-A1/SOX5 pathway that represents a promising therapeutic target for chemosensitizing LAD and provides predictive markers for evaluating the efficacy of chemotherapies. There are some limitations in our present study. For instance, the mechanism associated with the upregulation of FOX-A1 and SOX5 need to be further explored. The mechanism responsible for the interaction between FOX-A1 and SOX5 still

needs further investigation. We will investigate the molecular mechanism associated with FOX-A1/SOX5 axis in our future research.

Supplementary data to this article can be found online at https://doi.org/10.1016/j.ebiom.2019.05.046.

Acknowledgements

The authors thank the talents program of Jiangsu Cancer Hospital.

Conflicts of interest

The authors declare that there is no conflict of interest.

Author contribution

D.C., L.C., R.W., X.Z., and Z.Y.researched data. D.C., F.C., and C.Y. wrote the manuscript. J.F., H.Z., Z.Y., and L.C. reviewed and edited the manuscript. F.Y. and J.F. contributed to discussion of experimental design.

Funding

This work was supported by the National Natural Science Foundation of China (NO.81672928), Financial Grant from the China Postdoctoral Science Foundation (NO. 2018 T110466 and NO.2017 M621678), National Natural Science Foundation of China (NO.81702048, NO.81572345 and NO.81503528), the Suzhou Science and Technology Bureau project (No. SYS201609) and the Industrial Technology Innovation Project of Suzhou city (No. SYSD2016124). Funders had no influence on study design, data collection, data analysis, interpretation, writing of the report.

References

[1] Siegel RL, Miller KD, Jemal A. Cancer statistics, 2019. CA Cancer J Clin 2019;69(1):7–34.
[2] Liu K, Guo J, Liu K, Fan P, Zeng Y, Xu C, et al. Integrative analysis reveals distinct subtypes with therapeutic implications in KRAS-mutant lung adenocarcinoma. EbioMedicine 2018;36:196–208.
[3] Wang Z, Wei Y, Zhang R, Su L, Gogarten SM, Liu G, et al. Multi-Omics analysis reveals a HIF network and hub gene EPAS1 associated with lung adenocarcinoma. EbioMedicine 2018;32:93–101.
[4] Allemani C, Matsuda T, Di Carlo V, Harewood R, Matz M, Niksic M, et al. Global surveillance of trends in cancer survival 2000-14 (CONCORD-3): analysis of individual records for 37 513 025 patients diagnosed with one of 18 cancers from 322 population-based registries in 71 countries. Lancet 2018;391(10125):1023–75.
[5] Aisner DL, Sholl LM, Berry LD, Rossi MR, Chen H, Fujimoto J, et al. The impact of smoking and TP53 mutations in lung adenocarcinoma patients with targetable mutations-the lung Cancer mutation consortium (LCMC2). Clin Cancer Res 2018;24(5):1038–47.
[6] Riquelme E, Suraokar M, Behrens C, Lin HY, Girard L, Nilsson MB, et al. VEGF/VEGFR-2 upregulates EZH2 expression in lung adenocarcinoma cells and EZH2 depletion enhances the response to platinum-based and VEGFR-2-targeted therapy. Clin Cancer Res 2014;20(14):3849–61.
[7] Adderley H, Blackhall FH, Lindsay CR. KRAS-mutant non-small cell lung cancer: converging small molecules and immune checkpoint inhibition. EBioMedicine 2019;41:711–6.
[8] Garassino MC, Cho BC, Kim JH, Mazieres J, Vansteenkiste J, Lena H, et al. Durvalumab as third-line or later treatment for advanced non-small-cell lung cancer (ATLANTIC): an open-label, single-arm, phase 2 study. Lancet Oncol 2018;19(4):521–36.
[9] de Langen AJ, Smit EF. Therapeutic approach to treating patients with BRAF-mutant lung cancer: latest evidence and clinical implications. Ther Adv Med Oncol 2017;9(1):46–58.
[10] Denisov EV, Perelmuter VM. A fixed partial epithelial-mesenchymal transition (EMT) triggers carcinogenesis, whereas asymmetrical division of hybrid EMT cells drives cancer progression. Hepatology 2018;68(3):807–10.
[11] Simi AK, Anlas AA, Stallings-Mann M, Zhang S, Hsia T, Cichon M, et al. A soft microenvironment protects from failure of Midbody abscission and multinucleation downstream of the EMT-promoting transcription factor snail. Cancer Res 2018;78(9):2277–89.
[12] Zielinska HA, Holly JMP, Bahl A, Perks CM. Inhibition of FASN and ERalpha signalling during hyperglycaemia-induced matrix-specific EMT promotes breast cancer cell invasion via a caveolin-1-dependent mechanism. Cancer Lett 2018;419:187–202.
[13] Stavropoulou V, Kaspar S, Brault L, Sanders MA, Juge S, Morettini S, et al. MLL-AF9 expression in hematopoietic stem cells drives a highly invasive AML expressing EMT-related genes linked to poor outcome. Cancer Cell 2016;30(1):43–58.
[14] Wu YC, Tang SJ, Sun GH, Sun KH. CXCR7 mediates TGFbeta1-promoted EMT and tumor-initiating features in lung cancer. Oncogene 2016;35(16):2123–32.
[15] Maciaczyk D, Picard D, Zhao L, Koch K, Herrera-Rios D, Li G, et al. CBF1 is clinically prognostic and serves as a target to block cellular invasion and chemoresistance of EMT-like glioblastoma cells. Br J Cancer 2017;117(1):102–12.
[16] Chen D, Huang J, Zhang K, Pan B, Chen J, De W, et al. MicroRNA-451 induces epithelial-mesenchymal transition in docetaxel-resistant lung adenocarcinoma cells by targeting proto-oncogene c-Myc. Eur J Cancer 2014;50(17):3050–67.
[17] Werden SJ, Sphyris N, Sarkar TR, Paranjape AN, LaBaff AM, Taube JH, et al. Phosphorylation of serine 367 of FOXC2 by p38 regulates ZEB1 and breast cancer metastasis, without impacting primary tumor growth. Oncogene 2016;35(46):5977–88.
[18] Zhang X, Zhang L, Du Y, Zheng H, Zhang P, Sun Y, et al. A novel FOXM1 isoform, FOXM1D, promotes epithelial-mesenchymal transition and metastasis through ROCKs activation in colorectal cancer. Oncogene 2017;36(6):807–19.
[19] Kundu ST, Byers LA, Peng DH, Roybal JD, Diao L, Wang J, et al. The miR-200 family and the miR-183~96~182 cluster target Foxf2 to inhibit invasion and metastasis in lung cancers. Oncogene 2016;35(2):173–86.
[20] Li M, Yang J, Zhou W, Ren Y, Wang X, Chen H, et al. Activation of an AKT/FOXM1/STMN1 pathway drives resistance to tyrosine kinase inhibitors in lung cancer. Br J Cancer 2017;117(7):974–83.
[21] Hou Y, Zhu Q, Li Z, Peng Y, Yu X, Yuan B, et al. The FOXM1-ABCC5 axis contributes to paclitaxel resistance in nasopharyngeal carcinoma cells. Cell Death Dis 2017;8(3):e2659.
[22] Chen DQ, Pan BZ, Huang JY, Zhang K, Cui SY, De W, et al. HDAC 1/4-mediated silencing of microRNA-200b promotes chemoresistance in human lung adenocarcinoma cells. Oncotarget 2014;5(10):3333–49.
[23] Watanabe H, Ma Q, Peng S, Adelmant G, Swain D, Song W, et al. SOX2 and p63 colocalize at genetic loci in squamous cell carcinomas. J Clin Invest 2014;124(4):1636–45.
[24] Formisano L, Stauffer KM, Young CD, Bhola NE, Guerrero-Zotano AL, Jansen VM, et al. Association of FGFR1 with ERalpha maintains ligand-independent ER transcription and mediates resistance to Estrogen deprivation in ER(+) breast Cancer. Clin Cancer Res 2017;23(20):6138–50.
[25] Heinz S, Benner C, Spann N, Bertolino E, Lin YC, Laslo P, et al. Simple combinations of lineage-determining transcription factors prime cis-regulatory elements required for macrophage and B cell identities. Mol Cell 2010;38(4):576–89.
[26] Si H, Lu H, Yang X, Mattox A, Jang M, Bian Y, et al. TNF-alpha modulates genome-wide redistribution of DeltaNp63alpha/TAp73 and NF-kappaB cREL interactive binding on TP53 and AP-1 motifs to promote an oncogenic gene program in squamous cancer. Oncogene 2016;35(44):5781–94.
[27] Sissung TM, Baum CE, Deeken J, Price DK, Aragon-Ching J, Steinberg SM, et al. ABCB1 genetic variation influences the toxicity and clinical outcome of patients with androgen-independent prostate cancer treated with docetaxel. Clin Cancer Res 2008;14(14):4543–9.
[28] Zheng G, Zhang Z, Liu H, Xiong Y, Luo L, Jia X, et al. HSP27-mediated extracellular and intracellular signaling pathways synergistically confer Chemoresistance in squamous cell carcinoma of tongue. Clin Cancer Res 2018;24(5):1163–75.
[29] Zhang Z, Lin G, Yan Y, Li X, Hu Y, Wang J, et al. Transmembrane TNF-alpha promotes chemoresistance in breast cancer cells. Oncogene 2018;37(25):3456–70.
[30] Su S, Chen J, Yao H, Liu J, Yu S, Lao L, et al. CD10(+)GPR77(+) Cancer-associated fibroblasts promote Cancer formation and Chemoresistance by sustaining Cancer Stemness. Cell 2018;172(4):841–56 [e16].
[31] Xie SL, Fan S, Zhang SY, Chen WX, Li QX, Pan GK, et al. SOX8 regulates cancer stem-like properties and cisplatin-induced EMT in tongue squamous cell carcinoma by acting on the Wnt/beta-catenin pathway. Int J Cancer 2018;142(6):1252–65.
[32] Xu H, Lin F, Wang Z, Yang L, Meng J, Ou Z, et al. CXCR2 promotes breast cancer metastasis and chemoresistance via suppression of AKT1 and activation of COX2. Cancer Lett 2018;412:69–80.
[33] Yang K, Li Y, Lian G, Lin H, Shang C, Zeng L, et al. KRAS promotes tumor metastasis and chemoresistance by repressing RKIP via the MAPK-ERK pathway in pancreatic cancer. Int J Cancer 2018;142(11):2323–34.
[34] Lin L, Miller CT, Contreras JI, Prescott MS, Dagenais SL, Wu R, et al. The hepatocyte nuclear factor 3 alpha gene, HNF3alpha (FOXA1), on chromosome band 14q13 is amplified and overexpressed in esophageal and lung adenocarcinomas. Cancer Res 2002;62(18):5273–9.
[35] Du H, Chen Y, Hou X, Huang Y, Wei X, Yu X, et al. PLOD2 regulated by transcription factor FOXA1 promotes metastasis in NSCLC. Cell Death Dis 2017;8(10):e3143.
[36] Fu X, Jeselsohn R, Pereira R, Hollingsworth EF, Creighton CJ, Li F, et al. FOXA1 overexpression mediates endocrine resistance by altering the ER transcriptome and IL-8 expression in ER-positive breast cancer. Proc Natl Acad Sci U S A 2016;113(43):E6600–9.
[37] Renjie W, Haiqian L. MiR-132, miR-15a and miR-16 synergistically inhibit pituitary tumor cell proliferation, invasion and migration by targeting Sox5. Cancer Lett 2015;356(2 Pt B):568–578.
[38] Kurtsdotter I, Topcic D, Karlen A, Singla B, Hagey DW, Bergsland M, et al. SOX5/6/21 prevent oncogene-driven transformation of brain stem cells. Cancer Res 2017;77(18):4985–97.
[39] Hu J, Tian J, Zhu S, Sun L, Yu J, Tian H, et al. Sox5 contributes to prostate cancer metastasis and is a master regulator of TGF-beta-induced epithelial mesenchymal transition through controlling Twist1 expression. Br J Cancer 2018;118(1):88–97.
[40] Ma S, Chan YP, Woolcock B, Hu L, Wong KY, Ling MT, et al. DNA fingerprinting tags novel altered chromosomal regions and identifies the involvement of SOX5 in the progression of prostate cancer. Int J Cancer 2009;124(10):2323–32.
[41] Pei XH, Lv XQ, Li HX. Sox5 induces epithelial to mesenchymal transition by transactivation of Twist1. Biochem Biophys Res Commun 2014;446(1):322–7.